

Density functional study of atoms spatially confined inside a hard sphere

Sangita Majumdar and Amlan K. Roy*

*Department of Chemical Sciences, Indian Institute of Science Education and Research
Kolkata, Mohanpur-741246, Nadia, WB, India*

Abstract

An atom placed inside a cavity of finite dimension offers many interesting features, and thus has been a topic of great current activity. This work proposes a density functional approach to pursue both ground and excited states of a multi-electron atom under a spherically impenetrable enclosure. The radial Kohn-Sham (KS) equation has been solved by invoking a physically motivated work-function-based exchange potential, which offers near-Hartree-Fock-quality results. Accurate numerical eigenfunctions and eigenvalues are obtained through a generalized pseudospectral method (GPS) fulfilling the Dirichlet boundary condition. Two correlation functionals, *viz.*, (i) simple, parametrized local Wigner-type, and (ii) gradient- and Laplacian-dependent non-local Lee-Yang-Parr (LYP) functionals are adopted to analyze the electron correlation effects. Preliminary exploratory results are offered for ground states of He-isoelectronic series ($Z = 2 - 4$), as well as Li and Be atom. Several low-lying singly excited states of He atom are also reported. These are compared with available literature results—which offers excellent agreement. Radial densities as well as expectation values are also provided. The performance of correlation energy functionals are discussed critically. In essence, this presents a simple, accurate scheme for studying atomic systems inside a *hard* spherical box within the rubric of KS density functional theory.

PACS: 03.65-w, 03.65Ca, 03.65Ta, 03.65.Ge, 03.67-a.

Keywords: Quantum confinement, hard confinement, many-electron atom, density functional theory, exchange-correlation functional, generalized pseudospectral method.

*Corresponding author. Email: akroy@iiserkol.ac.in, akroy6k@gmail.com.

I. INTRODUCTION

In recent years, we have witnessed a proliferation of research activity in the field of quantum confinement. A particularly interesting situation arises when a spatial barrier causes dramatic changes in observable properties compared to their free counterpart. This type of perturbation deeply influences the ionization threshold, atomic size, molecular bond size, polarizability, energy spectrum etc. This remarkable difference in observed physico-chemical properties of two systems have motivated considerable amount of theoretical and experimental works in this direction. They have found significant relevance in modeling a large range of physical and chemical systems, *viz.*, calculation of zero-point energy in fluids at high density, description of magnetic behavior of metals under small magnetic field, restricted rotator, so-called *artificial atom* or quantum dot, matter (atom, molecule, ion), trapped atoms/molecules (inside cavity, zeolite channel, or in endohedral fullerene cage), etc. Particle in a box with impenetrable walls appears in some applications of acoustics and biology as well. Apart from the academic appeal, there is an underlying technological bearing in connection to the development of new materials with unconventional properties. The field is quite vast, relatively young and continuously expanding. Many excellent, elegant reviews are available. The interested reader may consult following works and references therein [1–4].

Different models were proposed in literature to probe the electronic structure of confined atoms. A simple intuitive one to represent this is to place the atom inside an impenetrable cavity of adjustable radius, whereby the electrostatic Hamiltonian is modified by adding a confining potential in terms of radius r_c . Ever since the seminal work on confined hydrogen atom (CHA) placed inside a hard spherical cage [5], this prototypical model was vigorously studied in reference to the eigenspectra, degeneracy pattern, static and dipole polarizability, nuclear magnetic screening constant, excited-state life time, pressure, hyperfine splitting constant, filling of electronic shells and many others. *Exact* analytical solution of CHA was reported [6] in terms of Kummer M -function (confluent hypergeometric). A huge amount of literature exists on the topic; they could be found from the references cited.

Confinement in *many-electron atom* becomes challenging due to the obvious presence of electron-electron Coulomb interaction, which breaks the $O(4)$ and $SU(3)$ symmetries of simplified one-electron system. This has generated considerable interest and curiosity to investigate the properties of a He atom centrally placed in a hard, rigid spherical cage. It

serves as a precursor to further atomic confinement studies. Energies as functions of r_c for a compressed He centered in a spherical impenetrable cavity was reported as early as in 1952 by a variational calculation [7]. Thereafter Roothaan Hartree-Fock (RHF) calculation with Slater-type basis functions [8], configuration interaction (CI) [9, 10], quantum Monte Carlo [11], direct variational [12–15], B-splines method [16], perturbation theory [14, 17], explicitly correlated Hylleraas-type wave functions within variational framework [18–25], a combination of quantum genetic algorithm and HF method [26], variational Monte Carlo [27, 28], HF calculation employing local and global basis sets [29], were adopted to produce better ground-state energies, ionization energies, critical cage, polarizability, hyperpolarizability, etc. Apart from the ground state, some low-lying excited states were also investigated. They include energies, polarizabilities and other properties in $1sns$ 1^3S [13, 14, 19, 22–26, 28, 30], $1s2p$ 1^3P [13, 26, 30], $1s3d$ 1^3D , and some doubly excited states [26, 30]. Note that spectroscopic properties of atoms under such spatially restricted environment not only involves ground state, but also essentially requires to probe the role played by excited states.

Similar to the confinement in one- and two-electron atoms, such studies were undertaken in other atoms in periodic table as well. Thus energy spectra of ground and excited states, as well as filling of shells in multi-electron atoms (more than two electrons) was investigated by means of a RHF-type calculation [8, 31], configuration average HF [32], HF [33], variational Monte Carlo [28], parameterized optimized effective potential (POEP) method using an appropriate cut-off factor [34], B-spline random phase approximation with exchange [35], explicitly correlated and multi-configuration variational method [36] and so on. The effect of confinement on correlation energy in case of atoms of first few rows were discussed [2, 3, 36–38]. Behavioral changes of compressed atoms under such very tight positions have been comprehensively reviewed by several researchers [39–41].

Apart from the methods mentioned above, there were attempts to pursue the problem through an alternate density functional theory (DFT). The ground states of a many-electron atom trapped in a spherical cavity was treated within an exchange-only framework (two functionals, *viz.*, local density approximation (LDA) [42] and Becke-88 exchange potential [43] were adopted); the radial Kohn-Sham (KS) equation was solved satisfying the Dirichlet boundary condition via numerical shooting method [44]. Later, ground and $1s2s$ ($3S$, $1S$) states of confined He were presented [45] by taking into consideration of LDA exchange-correlation (XC) (Perdew-Wang parametrization for correlation [46]), with and without

self-interaction correction (SIC). Reactivity indices like, electronegativity, global hardness, softness, HOMO-LUMO gap were been considered for ground state of such systems [47] using same XC potential. Similar study was performed by engaging Perdew-Burke-Ernzerhof (PBE) functional [48]. A DFT-based variation-perturbation approach [49] was proposed to calculate polarizability and hyperpolarizability in confined He. Lately, they were studied [50] via local exchange potentials approximated by Zhao-Morrison-Parr (ZMP) and Becke-Johnson (BJ) model. A correlation functional was designed involving the *ab initio* correlation energy density for confined atoms [51]. One-parameter hybrid exchange functional in the form of PBE exchange coupled with exact-exchange is applied for closed shell atoms inside penetrable and impenetrable cavity [52]. Recently, a DFT-based study was reported for confined first row transition metal cations [53]. Confinements within *penetrable* walls were undertaken [37] within a basis-set DFT for LDA and generalized-gradient approximated XC functionals. Apart from that, bonding, reactivity and dynamics of an atom encapsulated in fullerene cage is also investigated [54]. This discussion clearly suggests that, excluding a few cases, DFT calculations for confined atoms are restricted typically to ground state.

In this work, our objective is to present a general time-independent DFT scheme which can be applied for both ground as well as excited state of an atom, at any given radius of cavity. This is accomplished by invoking a simple, physically motivated work-function-based exchange potential [55, 56]. In order to include correlation effects, we adapt two correlation functionals, *viz.*, a simple, local, parametrized Wigner-type [57] and the other one, a slightly involved nonlinear Lee-Yang-Parr (LYP) [58] functional. This procedure was very successfully applied to a large number of excited states in *free* atoms, such as single, double, triple excitation; low- and high-lying excitation; valence as well as core excitation; hollow and satellite states; autoionizing and high-lying Rydberg states [59–64]. With this choice of XC functionals, the resultant KS equation is solved using the generalized pseudospectral (GPS) method imposing the appropriate boundary condition. Recently this has been successfully applied to estimate Shannon entropy in some low-lying states of confined He-isoelectronic series [65]. In this work, we focus on the so-called *hard* confinement of an arbitrary atom within a spherical rigid cavity, defined by radius r_c . This prescription is applicable to *soft or penetrable* boundary as well. A detailed systematic results on energy, density and selected expectation values are provided for ground and low-lying singly excited $1s2s\ ^3,^1S$, $1s2p\ ^3,^1P$, $1s3d\ ^3,^1D$ states of He; lowest states of Li^+ , Be^{2+} , as well as Li and Be atom. In order to

estimate the effects of correlation as well as to assess the performance of correlation energy functionals, both X-only and correlated results are given. Converged results are offered for low, intermediate and large r_c . Section II outlines the methodology used, Sec. III discusses the results along with comparison with literature, while Sec. IV draws a few conclusions.

II. METHODOLOGY

In this section, we first briefly outline the work-function methodology for an arbitrary state corresponding to an electronic configuration of a given atom. Then we discuss the GPS scheme employed for solution of target KS equation. Our starting point is the single-particle time-independent KS equation with imposed confinement, conveniently written as,

$$\mathbf{H}(\mathbf{r})\psi_i(\mathbf{r}) = \epsilon_i(\mathbf{r})\psi_i(\mathbf{r}), \quad (1)$$

where \mathbf{H} denotes the effective KS Hamiltonian, given by,

$$\begin{aligned} \mathbf{H}(\mathbf{r}) &= -\frac{1}{2}\nabla^2 + v_{eff}(\mathbf{r}) \\ v_{eff}(\mathbf{r}) &= v_{ne}(\mathbf{r}) + \int \frac{\rho(\mathbf{r}')}{|\mathbf{r} - \mathbf{r}'|} d\mathbf{r}' + \frac{\delta E_{xc}[\rho(\mathbf{r})]}{\delta \rho(\mathbf{r})} + v_{conf}(\mathbf{r}). \end{aligned} \quad (2)$$

Here $v_{ne}(\mathbf{r})$ signifies the external potential, whereas second and third terms in right-hand side represent classical Coulomb (Hartree) repulsion and XC potentials respectively. We assume here that the atom is placed at the center of a cavity of radius r_c with impenetrable surface which may be described by a potential of the form,

$$v_{conf}(\mathbf{r}) = \begin{cases} 0, & r \leq r_c \\ +\infty, & r > r_c. \end{cases} \quad (3)$$

Though DFT has achieved impressive success in explaining the electronic structure and properties of many-electron system in their ground state, calculation of excited-state energies and densities has remained somehow problematic. This is mainly due to the absence of a Hohenberg-Kohn theorem parallel to ground state, as well as the lack of a suitable XC functional valid for a general excited state. In this work, we have employed an accurate work-function-based exchange potential, $v_x(\mathbf{r})$, which is physically motivated. Accordingly, exchange energy can be interpreted as an interaction energy between an electron at \mathbf{r} and

its Fermi-Coulomb hole charge density $\rho_x(\mathbf{r}, \mathbf{r}')$ at \mathbf{r}' and given by [55, 56],

$$E_x[\rho(\mathbf{r})] = \frac{1}{2} \int \int \frac{\rho(\mathbf{r})\rho_x(\mathbf{r}, \mathbf{r}')}{|\mathbf{r} - \mathbf{r}'|} d\mathbf{r}d\mathbf{r}' \quad (4)$$

The assumption is such that a unique local potential exists for a particular state characterized by usual quantum numbers n, l, m . One can then define $v_x(\mathbf{r})$ as the work done in bringing an electron to the point \mathbf{r} against the electric field, $\mathcal{E}_x(\mathbf{r})$, produced by its Fermi-Coulomb hole density, and can be expressed as,

$$v_x(\mathbf{r}) = - \int_{\infty}^r \mathcal{E}_x(\mathbf{r}) \cdot d\mathbf{l}, \quad (5)$$

where

$$\mathcal{E}_x(\mathbf{r}) = \int \frac{\rho_x(\mathbf{r}, \mathbf{r}')(\mathbf{r} - \mathbf{r}')}{|\mathbf{r} - \mathbf{r}'|^3} d\mathbf{r}'. \quad (6)$$

The Fermi hole charge distribution is known precisely in terms of orbitals,

$$\rho_x(\mathbf{r}, \mathbf{r}') = - \frac{|\gamma(\mathbf{r}, \mathbf{r}')|^2}{2\rho(\mathbf{r})}, \quad (7)$$

and consequently the potential can be determined accurately. Here $|\gamma(\mathbf{r}, \mathbf{r}')| = \sum_i \phi_i^*(\mathbf{r})\phi_i(\mathbf{r}')$, is single-particle density matrix, $\phi_i(\mathbf{r})$ is single-particle orbital and $\rho(\mathbf{r})$ is electron density. Note that the potential does not have a definite functional form; the respective electronic configuration corresponding to a particular state defines it. In this sense this is universal, as the same equation is now valid for both ground and excited states. Now, the electron density can be obtained in terms of occupied orbitals as,

$$\rho(\mathbf{r}) = \sum_{i=1}^N |\psi_i(\mathbf{r})|^2. \quad (8)$$

For spherically symmetric systems, Eq. 6 can be simplified in the form [55, 56],

$$\begin{aligned} \mathcal{E}_{x,r}(r) &= \frac{1}{2\pi\rho(r)} \int \sum_{n,l,m,n',l',m',l''} R_{nl}(r)R_{nl}(r')R_{n'l'}(r)R_{n'l'}(r') \left[\frac{\partial}{\partial r} \frac{r_{\leq}^{l''}}{r_{>}^{l''+1}} \right] \\ &\times r'^2 dr' \frac{2l+1}{2l'+1} \times C^2(l'l'; m, m' - m, m') C^2(l'l'; 000), \end{aligned} \quad (9)$$

where $R_{nl}(r)$ denotes the radial part of orbitals, and C's signify Clebsch-Gordon coefficients.

It should be noted that this is an orbital dependent, non-variational method, which is applicable for both ground and excited states. The nagging orthogonality requirement of a given excited state with all other lower states of same space-spin symmetry is indirectly

bypassed. In this way, while $v_x(\mathbf{r})$ is incorporated correctly, one needs to approximate the correlation potentials. In present calculation, we have used simple Wigner [57] and slightly involved LYP [58] energy functionals to include correlation effects.

With the above choice of $v_x(\mathbf{r})$ and $v_c(\mathbf{r})$, the KS differential equation needs to be solved numerically maintaining self consistency. For an accurate and efficient solution, we have adopted the GPS method leading to a non-uniform, optimal spatial discretization. It is computationally orders of magnitude faster than the traditional finite-difference methods. The characteristic feature of this method lies in approximating an *exact* function $f(x)$, defined in a range $[-1, 1]$, by an N th-order polynomial $f_N(x)$,

$$f(x) \cong f_N(x) = \sum_{j=0}^N f(x_j)g_j(x), \quad (10)$$

and ensure the estimation to be *exact* at *collocation points* x_j ,

$$f_N(x_j) = f(x_j). \quad (11)$$

The radial domain of the atom constrained within a sphere of radius r_c ($r \in [0, r_c]$) is mapped onto the finite interval $[-1, 1]$ via the following algebraic nonlinear mapping function,

$$r = r(x) = L \frac{1+x}{1-x+\alpha}, \quad (12)$$

where L and $\alpha = 2L/r_c$ are two mapping parameters.

Here we employ the Legendre pseudo-spectral method requiring $x_0 = -1$, $x_N = 1$, whereas x_j ($j = 1, \dots, N-1$) are defined by the roots of first derivative of Legendre polynomial $P_N(x)$, with respect to x , namely,

$$P'_N(x_j) = 0. \quad (13)$$

In Eq. (10), $g_j(x)$ are termed *cardinal functions*, and as such, are given by,

$$g_j(x) = -\frac{1}{N(N+1)P_N(x_j)} \frac{(1-x^2)P'_N(x)}{(x-x_j)}, \quad (14)$$

fulfilling the unique property that, $g_j(x_{j'}) = \delta_{j',j}$. Then use of a non-linear mapping followed by a symmetrization procedure, eventually leads to a symmetric eigenvalue problem, which can be solved by readily standard softwares to provide accurate eigenvalues and eigenfunctions. The intermediate steps and other details have been discussed at length in several publications (see e.g., [62–64, 66, 67] and references therein); hence they are omitted here.

Now, our desired confinement is introduced by requiring that the total electron density vanishes at the boundaries of spherical cavity that surrounds an atom, which is achieved by imposing the boundary condition, $\psi_{nl}(0) = \psi_{nl}(r_c) = 0$. The self-consistent orbitals can be used to construct relevant Slater determinants corresponding to a specific electronic configuration, from which multiplet energies can be estimated following Slater’s diagonal sum rule [59–64, 68].

It is worth mentioning here that, in literature, majority works deal with moderate to large r_c region; much fewer papers have been devoted to smaller r_c . As, in this work, we have not faced any extra difficulty to obtain converged solution in latter scenario, we are able to consider all strengths of confinement with uniform accuracy and ease, quite comfortably. A general convergence criteria in energy (10^{-6}) and potential (10^{-5}) during the iterative process, as well as GPS parameters (radial grid point, $n_r = 300, L = 1$) were employed throughout the whole confinement region, and for all states undertaken here.

III. RESULT AND DISCUSSION

In the following, non-relativistic energies, radial expectation values and radial densities will be reported for ground and low-lying singly excited $1s2s\ ^3,^1S$, $1s2p\ ^3,^1P$, $1s3d\ ^3,^1D$ states of a confined He atom. Then these are extended for the ground states of He-isoelectronic series ($Z = 2 - 4$), as well as Li and Be atom. All results are given in atomic units, unless stated otherwise. To put things in proper perspective, three sets of energies are offered, *viz.*, (i) exchange-only (ii) considering Wigner correlation (iii) including LYP correlation. Throughout the discussion, these are abbreviated as X-only, XC-Wigner and XC-LYP. Some of these states (especially first few low-lying ones) are amongst the heavily studied cases for confined many-electron atoms. Consequently many authors have studied them and these are quoted wherever feasible.

A. Confined He atom

Let us first discuss ground-state energies of confined He in Table I, for 15 representative r_c ’s, starting from a very strong confinement in $r_c = 0.1$ to a large r_c , corresponding to *free* atom. This is the most vigorously studied case, as it bears relevance to the simplest

TABLE I: Ground-state energy of radially confined He for different r_c . See text for details.

r_c	X-only	Literature	XC-Wigner	XC-LYP	Literature
0.1	906.61645		906.44963	907.45572	906.6575 ^s
0.2	206.20456		206.06251	206.67838	206.1696 ^s
0.5	22.79096	22.79095 ^a , 22.79096 ^p , 23.32202 ^q , 22.80168 ^w	22.69096	22.95926	22.7437 ^c , 22.7413 ^m , 22.741303 ⁿ , 23.099 ^r , 22.7423 ^s , 22.70203 ^u
0.6	13.36683	13.36682 ^a , 13.36683 ^p , 13.81792 ^q , 13.36759 ^w	13.27536	13.49338	13.3204 ^c , 13.318340 ^h , 13.3343 ⁱ , 13.3182 ^m , 13.605 ^r , 13.3186 ^s , 13.31194 ^u
0.8	4.65737	4.65737 ^a , 4.6610 ^b , 4.65736 ^p , 5.00895 ^q , 4.65760 ^w	4.57870	4.72898	4.6225 ^b , 4.6125 ^c , 4.610554 ^h , 4.6157 ⁱ , 4.6104 ^m , 4.8133 ^r , 4.6105 ^s , 4.640665 ^u
1	1.06121	1.06122 ^a , 1.0625 ^b , 1.354 ^e , 1.112 ^f , 1.06120 ^{o, p, w} , 1.35362 ^q	0.99159	1.09882	1.0186 ^b , 1.0176 ^c , 1.0142 ^d , 1.015870 ^h , 1.0183 ⁱ , 1.0158 ^{m, s} , 1.015755 ^{n, o} , 1.17040 ^r , 1.01690 ^t
1.2	-0.66461	-0.66461 ^a , -0.6639 ^b , -0.66458 ^w	-0.72758	-0.64954	-0.7075 ^b , -0.7070 ^c , -0.708716 ^h , -0.7079 ⁱ , -0.7088 ^m , -0.7087 ^s , -0.70747 ^t , -0.708609 ^u , -0.708801 ^v
1.4	-1.57416	-1.57417 ^{a, w} , -1.5741 ^b	-1.63213	-1.57468	-1.6151 ^b , -1.6156 ^c , -1.60119 ^g , -1.617154 ^h , -1.6167 ⁱ , -1.6173 ^m , -1.6172 ^s , -1.61569 ^t , -1.616875 ^u
1.5	-1.86422	-1.8642 ^b , -1.86422 ^p , -1.64897 ^q	-1.92015	-1.87072	-1.9040 ^b , -1.9081 ^d , -1.69149 ^g , -1.906740 ^h , -1.9061 ⁱ , -1.81185 ^r , -1.9067 ^s , -1.90599 ^t , -1.906956 ^v
2	-2.56256	-2.56253 ^a , -2.5594 ^b , -2.384 ^e , -2.542 ^f , -2.56258 ^j , -2.56257 ^{p, w} , -2.39363 ^q	-2.61154	-2.58790	-2.5977 ^b , -2.6026 ^c , -2.6051 ^d , -2.5028 ^g , -2.603630 ^h , -2.5998 ⁱ , -2.60403 ^{k, n} , -2.62589 ^l , -2.6040 ^m , -2.53480 ^r , -2.6036 ^s , -2.60223 ^t , -2.604038 ^v
3	-2.83103	-2.83083 ^a , -2.8232 ^b , -2.682 ^e , -2.826 ^f , -2.83105 ^j , -2.83078 ^p , -2.68201 ^q , -2.83099 ^w	-2.87460	-2.86888	-2.8652 ^b , -2.8708 ^c , -2.8727 ^d , -2.86849 ^g , -2.871808 ^h , -2.8636 ⁱ , -2.87426 ^k , -2.89038 ^l , -2.8725 ^m , -2.872495 ⁿ , -2.82256 ^r , -2.8718 ^s , -2.872494 ^v
4	-2.85856	-2.85852 ^a , -2.8537 ^b , -2.718 ^e , -2.859 ^f , -2.85859 ^j , -2.85854 ^p , -2.71807 ^q , -2.85834 ^w	-2.90093	-2.89939	-2.8956 ^b , -2.8988 ^c , -2.9003 ^d , -2.899687 ^h , -2.8931 ⁱ , -2.90042 ^k , -2.91691 ^l , -2.9004 ^m , -2.900485 ⁿ , -2.85552 ^r , -2.8997 ^s , -2.89834 ^t , -2.894997 ^u , -2.900486 ^v
5	-2.86136	-2.86134 ^a , -2.8589 ^b , -2.723 ^e , -2.863 ^f , -2.86139 ^{j, o} , -2.86138 ^p , -2.72288 ^q , -2.86129 ^w	-2.90352	-2.90332	-2.9004 ^b , -2.9020 ^c , -2.9032 ^d , -2.8764 ^g , -2.8978 ⁱ , -2.90337 ^k , -2.91951 ^l , -2.9034 ^m , -2.903410 ^{n, v} , -2.903409 ^o , -2.85856 ^r , -2.9028 ^s , -2.903886 ^u
6	-2.86162	-2.86151 ^a , -2.724 ^e , -2.863 ^f , -2.86165 ^j , -2.86162 ^p , -2.72346 ^q	-2.90376	-2.90422	-2.9024 ^c , -2.9035 ^d , -2.903278 ^h , -2.8990 ⁱ , -2.90368 ^k , -2.91975 ^l , -2.9037 ^m , -2.903696 ⁿ , -2.86000 ^r , -2.9033 ^s , -2.90190 ^t , -2.903460 ^u
∞	-2.86164	-2.86165 ^a , -2.8615 ^b , -2.861680 ^o , -2.86168 ^{j, w}	-2.90378	-2.90644	-2.9024 ^b , -2.9025 ^c , -2.9037 ^d , -2.8764 ^g , -2.903513 ^h , -2.8999 ⁱ , -2.90372 ^k , -2.91977 ^l , -2.9037 ^{m, s} , -2.903724 ^{n, o, v} , -2.90201 ^t

^aRef. [8].

^bRef. [69].

^cRef. [9].

^dRef. [11].

^eLSDA result of [44].

^fB88 result of [44].

^gRef. [10].

^hRef. [18].

ⁱRef. [13].

^jX-only, LDA-SIC result of [45].

^kVariational result of [45].

^lLDA-SIC result of [45].

^mRef. [19].

ⁿRef. [20].

^oRef. [21].

^pExact exchange result of [49].

^qX-only LDA result of [49].

^rXC-LDA result of [49].

^sRef. [14].

^tRef. [15].

^uRef. [27].

^vRef. [23].

^wRef. [26].

prototypical many-electron atom. The X-only results are compared with available literature by tabulating them in column 3. The RHF energies [8] within a Clementi-Roetti basis, are found for all r_c except 0.1, 0.2, 1.5. For the entire region of confinement, present results of column 2 show excellent agreement. Note that, in several instances, the two energies are identical. A similar agreement is also noticed for the exact exchange result (denoted by EXX in Table I of [49]) throughout the entire r_c . Apart from these two cases, another reference pertaining to this case includes HF [21, 69]. The X-only result (XO-LDA of [49]) employing local Dirac exchange functional [70], are also linked in present scenario. Generally, these energies remain consistently above our X-only result. The discrepancy is more prominent in lower r_c 's, with absolute deviation hovering within the range 2.3-21.6%. Similar calculations within LDA by various researchers [44, 45, 49] are also referred. The inclusion of SIC in LDA X-only framework [45] improves energies and at larger r_c , it yields values close to HF. Present X-only scheme performs better compared to LDA. A GGA-based DFT [44] using B88 functional [43], provides better approximation to HF than LDA. Our scheme provides appreciable agreement with GGA results. It is necessary to mention that, at strong confinement ($r_c < 4$) region these GGA energies are higher relative to the present case. However, at large r_c , a reverse situation is noticed. A slightly compromised matching is observed with [26], where a combination of quantum genetic algorithm and RHF is utilized.

Columns 4, 5 of Table I now report XC-Wigner and XC-LYP energies, along with literature results in column 6. The differences in two energies remain in the range of 0.0002-1.006 a.u. In free-limit scenario, the two energies come quite closer. References are more prevalent for $r_c \geq 0.5$ than $r_c < 0.5$. In general, from *free* atom, at $r_c \rightarrow \infty$, compression of the box is accompanied by an increase in energy. Overall energy comprises two terms, namely, confinement kinetic and Coulomb interaction energy. As an atom is enclosed, it gets constrained in a shorter box, leading to a net accumulation of kinetic energy. For all r_c 's, energies can be compared with that of [14], involving a wave function expanded via a generalized Hylleraas basis (GHB) (10 terms) along with a suitable cut-off factor. Both Wigner and LYP functionals produce reasonably good agreement with these, recording absolute deviations of 0.02-9.23% and 0.01-8.35%. In strong to moderate zone, energies distinctly remain nearer to XC-Wigner; however with an enhancement of box size, three energies eventually tend to approach each other closely. A 25-term variational function in a GHB with a cut-off function [19, 45] generally gives energies in between the two functionals; discrepancies range

TABLE II: Energy values of $1s2s\ ^3,^1S$ states of He confined in a spherical cavity of radius r_c .

r_c	3S				1S			
	X-only	XC-Wigner	XC-LYP	Literature	X-only	XC-Wigner	XC-LYP	Literature
0.1	2370.7389	2370.5729	2372.1569	2388.7273 ^b ,2370.8673 ^c	2376.4826	2376.3166	2377.9005	1995.2692 ^b ,2376.8368 ^c
0.2	568.19924	568.05832	569.03586	572.3488 ^b ,568.2066 ^c	571.14431	571.00342	571.98094	485.3350 ^b ,571.1854 ^c
0.3	241.50286	241.37997	242.08839	243.1949 ^b ,241.5068 ^c	243.51696	243.39410	244.10248	209.3899 ^b ,243.5355 ^c
0.5	78.83157 79.43685 ^a	78.73300	79.17557	79.3341 ^b ,78.8352 ^c	80.10411 79.65350 ^a	80.00552	80.44798	70.6581 ^b ,80.1154 ^c
0.6	51.86713 52.23345 ^a	51.77718	52.14254	52.1803 ^b ,51.8709 ^c	52.95550 52.68074 ^a	52.86571	53.23094	47.4173 ^b ,52.9658 ^c
0.8	25.86532 26.06405 ^a	25.78841	26.04941	26.0029 ^b ,25.8693 ^c	26.72502 26.14839 ^a	26.64834	26.90914	24.8168 ^b ,26.7338 ^c
1	14.36896 14.43401 ^a	14.30144	14.49546	15.5451 ^d ,14.3598 ^e , 14.3599 ^b ,14.3733 ^c	15.09248 14.87847 ^a	15.02498	15.21902	14.5358 ^b ,15.0998 ^c
1.5	3.81468	3.76201	3.86349	3.8068 ^b ,3.8199 ^c	4.3546	4.30191	4.40345	4.3045 ^b ,4.3567 ^c
2	0.56698 0.56961 ^a , 0.56698 ^f	0.52281	0.57954	0.5862 ^d ,0.56026 ^h , 0.58463 ⁱ ,0.5603 ^{e,b} , 0.5733 ^c	1.0021 0.60713 ^a , 0.99333 ^f	0.95795	1.0146	0.9639 ^b ,0.9977 ^c
2.5	-0.74592	-0.78479	-0.75220	-0.7516 ^e , -0.751657 ^g	-0.39500	-0.43469	-0.40158	-0.433214 ^j
3	-1.36562 -1.36799 ^a , -1.36605 ^f	-1.40091	-1.38218	-1.3679 ^d , -1.37046 ^h , -1.34861 ⁱ , -1.3705 ^{e,b} , -1.3562 ^c	-1.09026 -1.34955 ^a , -1.08419 ^f	-1.12545	-1.10734	-1.0991 ^b , -1.0937 ^c , -1.114121 ^j
4	-1.87095 -1.87331 ^a , -1.87162 ^f	-1.90207	-1.89643	-1.8734 ^d , -1.87461 ^h , -1.86296 ⁱ , -1.8746 ^{e,b} , -1.8569 ^c , -1.874612 ^g	-1.70881 -1.86047 ^a , -1.70025 ^f	-1.73987	-1.73465	-1.6949 ^b , -1.6913 ^c
5	-2.04515 -2.04787 ^a , -2.04590 ^f	-2.07406	-2.07324	-2.0473 ^d , -2.04804 ^h , -2.04317 ⁱ , -2.0480 ^{e,b} , -2.0250 ^c , -2.048044 ^g	-1.94379 -1.94676 ^a , -1.93612 ^f	-1.97274	-1.97136	-1.8684 ^b , -1.9051 ^c , -1.949761 ^j
6	-2.11539 -2.11615 ^f	-2.14302	-2.14389	-2.1171 ^d , -2.11782 ^h , -2.11609 ⁱ , -2.1178 ^{e,b} , -2.0880 ^c	-2.04408 -2.04168 ^f	-2.07167	-2.07084	-1.9136 ^b , -1.9880 ^c
10	-2.17079 -2.17146 ^a	-2.19663	-2.19745	-2.1714 ^d , -2.17262 ^h , -2.17345 ⁱ , -2.1726 ^e , -2.172627 ^g	-2.12726 -2.13092 ^a	-2.15583	-2.15087	-2.139619 ^j
∞	-2.17342 -2.17424 ^f	-2.19990	-2.19918	-2.17523 ^h , -2.1752 ^{e,b} , -2.17622 ⁱ , -2.1241 ^c	-2.13488 -2.14340 ^f	-2.16928	-2.15214	-1.9264 ^b , -2.0364 ^c , -2.145974 ^j

^aRef. [26].

^bGH result of [14].

^cPT result of [14].

^dRef. [13].

^eRef. [19].

^fRef. [71].

^gRef. [25].

^hVariational result of [45].

ⁱLDA-SIC result of [45].

^jRef. [23].

in between 0.002-2.65% and 0.003-8.36%, indicating slight advantage of Wigner correlation. Except for first two box sizes and $r_c = 1.5$, these were systematically estimated as early as in 1979 in [9] using a 41-term CI expansion generated by a 6s4p4d basis. In moderate to smaller box size ($r_c < 3$) these correlated reference results seem to be reproduced better by Wigner than LYP; after that the three energies tend to corroborate each other. The calculated energies are also compared with CI method involving HB [10, 20]. The variational Monte Carlo energies [27] (with a set of 10^6 points), by and large, maintain similar agreement with two correlation functionals, as the previous two, except for r_c of 0.5 a.u., where it gives an underestimation by about 0.04 a.u. Quantum Monte Carlo energies [11], (for $1 \leq r_c \leq 2.5$), show better consensus with Wigner than LYP. For $r_c \geq 1$, the Rayleigh-Ritz calculation [15] also provides similar conclusions as above references, leading to deviations of 0.06-2.84%, 0.04-8.19% for Wigner and LYP. Except for first two r_c 's, energies were published [13] from a two-parameter, correlated two-particle variational function; two functionals differ by 0.16-2.78% and 0.18-8.22%. The KS DFT [49], with an STO basis, consistently produces higher energies than both XC-Wigner (by 1.53-15.28%) and XC-LYP (by 0.61-6.12%). The LDA XC energies with SIC published in [45] show decent agreement for intermediate to large r_c .

Next, we apply this method in case of excited states. This gives an opportunity to test and assess its performance in such states under hard confinement. Thus Table II furnishes energies of singly excited $1s2s$ 3S and 1S states of a caged-in He atom for a wide range of r_c . Reference theoretical results in this situation are not as diverse as in previous table; nevertheless a substantial amount exists, which are duly given in footnote. The presentation strategy remains same as before. X-only energies for triplet, singlet states are tabulated at different r_c 's in columns 2, 6 respectively, along with RHF result (for $r_c \geq 0.5$) within an STO basis and invoking a genetic algorithm for minimization [26]. Triplet energies remain lower by 0.45-0.76% when radius remains below 2, while they lie 0.03-0.46% above reference otherwise. For singlet state, however, current energies are uniformly overestimated (0.17-65.1%) throughout the whole strength. In singlet case, $r_c \geq 2$ region records maximum deviation. This large discrepancy is rather unexpected and unusual, as none of our X-only results in preceding (for ground state) and any of the future tables (as will be evident from discussion later) produces this kind of differences when compared to other accurate theoretical methods. Moreover, very recently, a multi-configuration parametrized optimized effective potential (POEP) method [71] has been proposed for both these states for $r_c \geq 2$,

TABLE III: Singly-excited $1s2p\ ^3P$ and $1s3d\ ^3D$ energies of He at various r_c , in a.u.

r_c	$1s2p\ ^3P$					$1s2p\ ^1P$				
	X-only	Lit.	XC-Wigner	XC-LYP	Lit.	X-only	Lit.	XC-Wigner	XC-LYP	Lit.
0.1	1429.4156		1429.2504	1430.4981		1436.5840		1436.4189	1437.6666	
0.5	45.01798	45.06318 ^a	44.9220	45.2679		46.4261	46.48432 ^a	46.3302	46.6761	
0.8	13.83774	13.84936 ^a	13.7638	13.9646		14.7012	14.71138 ^a	14.6274	14.8281	
1	7.18913	7.19649 ^a , 7.18908 ^b	7.1246	7.2717	7.5265 ^d , 7.680 ^e	7.8689	7.87081 ^a , 7.86331 ^b	7.8045	7.9515	8.0312 ^d , 7.751 ^e
1.6	0.69311	0.69364 ^a	0.6453	0.7089		1.0894	1.08013 ^a	1.0417	1.1053	
1.8	-0.06149	-0.06022 ^a	-0.1059	-0.0572		0.2798	0.26860 ^a	0.2354	0.2841	
2	-0.56852	-0.56750 ^a , -0.56854 ^{b,c}	-0.6102	-0.5729	-0.4907 ^d , -0.3692 ^e	-0.2722	-0.42358 ^a , -0.28495 ^{b,c}	-0.3139	-0.2767	-0.3414 ^d , -0.3334 ^e
5	-2.01896	-2.01930 ^a , -2.01977 ^{b,c}	-2.0475	-2.0506	-2.0126 ^d , -2.0012 ^e	-1.9631	-1.99797 ^a , -1.98051 ^{b,c}	-1.9909	-1.9938	-1.9928 ^d , -1.9857 ^e
7	-2.0991	-2.10041 ^a , -2.10049 ^{b,c}	-2.1255	-2.1290	-2.0964 ^d , -2.0934 ^e	-2.0677	-2.11382 ^a , -2.08193 ^{b,c}	-2.0930	-2.0953	-2.0861 ^d , -2.0812 ^e
10	-2.12479	-2.12665 ^a , -2.12644 ^{b,c}	-2.1497	-2.1518	-2.1234 ^d , -2.1249 ^e	-2.1023	-2.11563 ^a , -2.11566 ^{b,c}	-2.1258	-2.1255	-2.1172 ^d , -2.1146 ^e
	$1s3d\ ^3D$					$1s3d\ ^1D$				
0.1	2086.2494		2086.0853	2087.5813		2089.0937		2088.9296	2090.4256	
0.5	72.18395	72.30233 ^a	72.0901	72.5138		72.7197	72.75302 ^a	72.6260	73.0497	
1	14.26227	14.28253 ^a	14.2000	14.3867		14.5037	14.40101 ^a	14.4415	14.6282	
2	1.33071	1.33232 ^a	1.2910	1.3444		1.4151	1.37266 ^a	1.3753	1.4289	
2.2	0.66672	0.66777 ^a	0.6291	0.6716		0.7361	0.73500 ^a	0.6984	0.7407	
2.6	-0.20070	-0.19987 ^a	-0.2350	-0.2079		-0.15415	-0.15599 ^a	-0.18889	-0.1615	
3	-0.72396	-0.72362 ^a	-0.7562	-0.7385		-0.6930	-0.70951 ^a	-0.7255	-0.7077	
5	-1.67291	-1.67325 ^a	-1.7001	-1.6975		-1.6684	-1.61835 ^a	-1.6959	-1.6931	
7	-1.9037	-1.9038 ^a	-1.9290	-1.9272		-1.9026	-1.9035 ^a	-1.9281	-1.9261	
10	-2.00707	-1.98617 ^a	-2.0310	-2.0218		-2.0068	-2.00707 ^a	-2.0308	-2.0213	

^aRef. [26].

^bRef. [72].

^cRef. [71].

^dRef. [13].

^eRef. [73].

which offers excellent agreement with X-only energies recording 0.001-0.03% and 0.11-0.88% of absolute deviations; in a few instances, two energies completely merge. Thus, on the light of above facts, we are confident that present energies are better than those of [26]; more careful and sophisticated calculations in future will hopefully resolve this issue. Now coming to correlated scenario, accurate variational energies [14, 19, 23, 45] by choosing a variety of large expansions in HB are available. These references, more or less, remain in conformity with each other. For singlet state, these can be compared with the accurate correlated wave function with 161 terms in HB [23]. Here our energies (both Wigner and LYP) are underestimated, except for XC-LYP at $r_c \leq 3$ where it is overestimated. Another

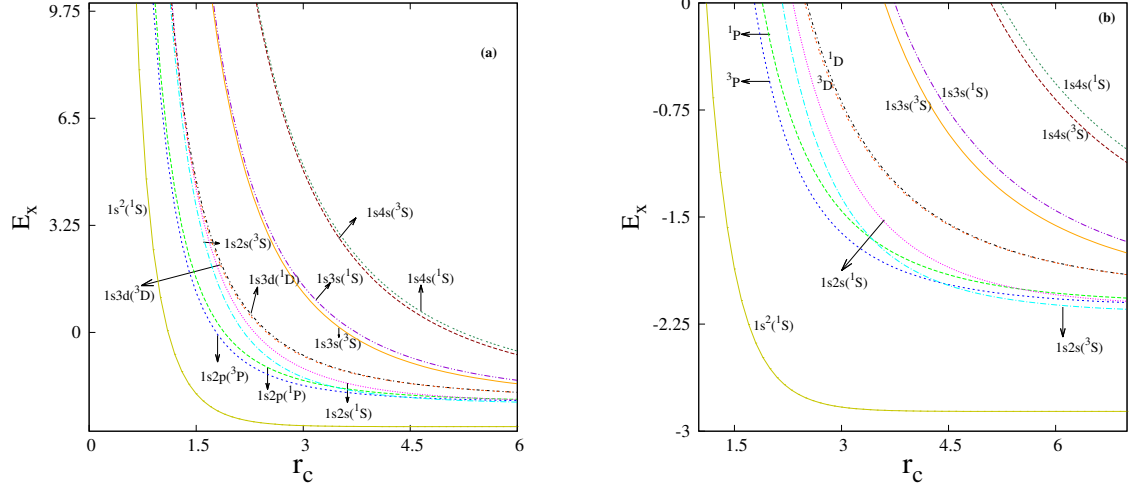


FIG. 1: Energy changes in some low-lying states of confined He with r_c in (a). Panel (b) shows a magnification of (a) in $E \leq 0$ region. See text for details.

reference is due a perturbative approach [14], for both states at all r_c 's except at 2.5 and 10. It records absolute error in ranges of 0.02-3.56%, 0.05-3.53% for triplet, while 0.02-6.52%, 0.04-5.68% for singlet, with Wigner and LYP functionals. Triplet energies obtained by solving KS equation with LDA and LDA-SIC [45] differ considerably from each other and also from other variational results, for all $r_c \geq 2$. For higher- S state, accurate energies are also available from Ritz method using an explicitly correlated HB [25], for all $r_c \geq 2.18$ a.u.

In order to augment the discussion on excited states, Table III next offers specimen triplet and singlet energies of confined He corresponding to states having total orbital angular momentum $L = 1, 2$ arising from singly excited configurations $1s2p$ and $1s3d$. Maintaining consistency with earlier presentation strategy, X-only results are tabulated in 2nd and 7th columns in upper ($1s2p$) and lower ($1s3d$) sections, at representative r_c 's. As before, energies monotonically fall off as the box is enlarged. Literature results in these cases are visibly scarce. For $r_c \geq 0.5$, STO-based RHF [26] shows, in general, nice agreement with X-only values for entire range, excepting some stray cases where, as in previous table, some spike is observed. Thus, while 3P remains within 0.02-2.02%, 1P is estimated within 0.02-4.17%, excepting the special case for $r_c = 2$, where an unusually large difference of 35.73% is recorded. For $^3,^1P$, near-HF energies within a POEP method has been reported lately [72], for $r_c \geq 1$. It is encouraging to note that, for 3P , our energies match excellently with theirs, uniformly for all radii. However, for 1P , current energies remain slightly higher when $r_c < 5$,

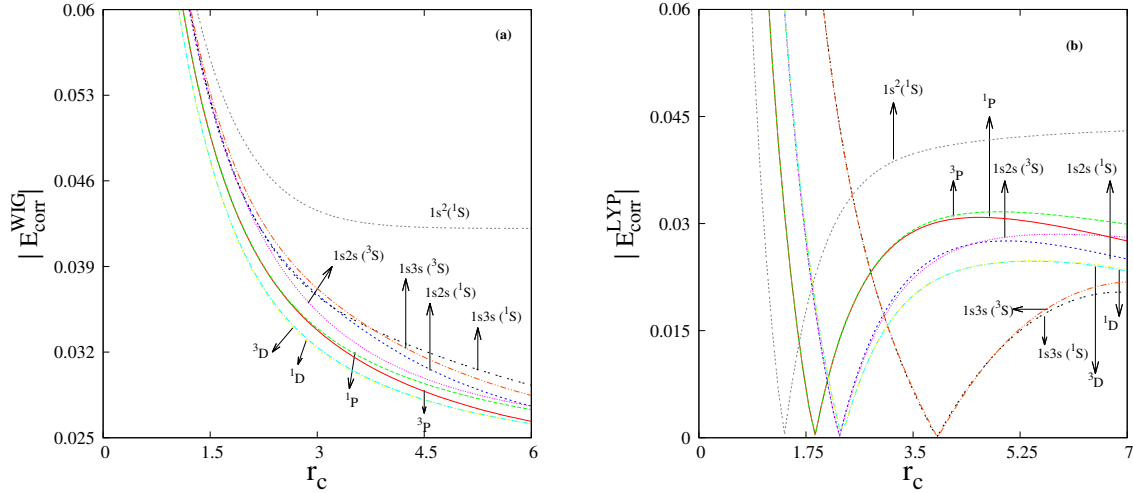


FIG. 2: Absolute value of correlation energies for singly excited states of confined He, in panels (a) and (b) for Wigner and LYP functionals, with changes in box size. See text for details.

but steadily lowers as we approach the free-atom unconfined limit. These reference results also fully match with [71], for all available r_c . Absolute deviation relative to [72] lies in the range of 0.001-0.08% and 0.07-4.47% for 3P , 1P . The correlated 3P energies are found to be lower for both functionals throughout entire strength with respect to the interpolation approach of [73] and variational scheme [13]. But for 1P , present energies are lower in small r_c , while producing higher values in moderate to large r_c . The energy difference between two functionals gradually diminishes as confinement occurs in larger enclosures. For D states, X-only results give absolute deviations of 0.005-1.05% and 0.01-3.1% for 3D and 1D . No literature data can be found for correlated energies, for direct comparison. Moreover, no DFT calculations are known for any of these states in this table.

In order to illustrate the impact of confinement, energies of compressed He are portrayed in panels (a) and (b) of Fig. 1 for a few selected singlet and triplet singly excited states as a function of r_c . In addition to the states considered in above tables, here we also include $1s3s$ and $1s4s$ $^3,^1S$. To get a better understanding of crossing amongst various states, a magnified portion of (a) is displayed in (b) in the negative energy region, with improved resolution. Since X-only, XC-Wigner, XC-LYP energies produce qualitatively similar plots, we have taken liberty to use X-only energies to illustrate the essential features. In consonance with discussions of Tables I-III, here also it is evident that, while influence of $v_{conf}(\mathbf{r})$ seems to be

TABLE IV: Energy difference and contribution of various components in the pair of states ($1s2s^3S$, $1s2p^3P$) and ($1s3d^3D$, $1s2s^3S$) for confined He atom at different r_c 's. See text for details.

(1s2p 3P , 1s2s 3S)								
	$r_c = 0.1$	$r_c = 0.3$	$r_c = 0.7$	$r_c = 1$	$r_c = 2.5$	$r_c = 4.4$	$r_c = 4.5$	$r_c = 20$
$\Delta E_{(3P-3S)}$	-941.3233	-99.3402	-16.2298	-7.1798	-0.5294	-0.0004	0.0054	0.0437
$\Delta T_{(3P-3S)}$	-964.5660	-107.3300	-19.8379	-9.7766	-1.4554	-0.2810	-0.2603	-0.0425
$\Delta V_{\text{en}(3P-3S)}$	25.5989	8.7414	3.8949	2.7744	0.9275	0.2415	0.2265	0.0745
$\Delta V_{\text{ee}(3P-3S)}$	-2.3561	-0.7517	-0.2868	-0.1776	-0.0015	0.0390	0.0391	0.0117
(1s3d 3D , 1s2s 3S)								
	$r_c = 0.1$	$r_c = 0.3$	$r_c = 0.5$	$r_c = 1$	$r_c = 1.1$	$r_c = 5$	$r_c = 10$	$r_c = 30$
$\Delta E_{(3D-3S)}$	-284.4894	-63.8781	-6.6476	-0.1066	0.1746	0.3722	0.1637	0.1180
$\Delta T_{(3D-3S)}$	-313.2606	-78.4721	-12.7192	-3.2871	-2.7324	0.0841	-0.0155	-0.1154
$\Delta V_{\text{en}(3D-3S)}$	30.0266	15.2141	6.3092	3.2885	3.0031	0.3321	0.2772	0.3948
$\Delta V_{\text{ee}(3D-3S)}$	-1.2554	-0.6200	-0.2376	-0.0959	-0.0440	-0.0259	-0.0980	-0.1613

more effective in smaller r_c in low-lying states, for higher states this impact causes a shift towards larger r_c . In *free* He atom, the ordering of states under consideration is: $E_{1s4s(1S)} > E_{1s4s(3S)} > E_{1s3d(3D)} > E_{1s3d(1D)} > E_{1s3s(1S)} > E_{1s3s(3S)} > E_{1s2p(1P)} > E_{1s2p(3P)} > E_{1s2s(1S)} > E_{1s2s(3S)} > E_{1s^2(1S)}$. With increase in confinement strength, this ordering gets dissolved due to multiple crossing between states, and rearrangement that occurs therefrom; it becomes function of r_c . Thus at $r_c \approx 5.3$, 4.45, 3.4, crossings occur between $1s2p^1P$, $1s2s^1S$; $1s2p^3P$, $1s2s^3S$; $1s2p^1P$, $1s2s^3S$ respectively. It is to be mentioned that, beyond the limits of r_c presented here, several other crossings occur, which are not shown in this figure, to avoid clumsiness. This point will be further taken up in later part of this section.

From the foregoing analysis, it is obvious that energies of a confined He are less sensitive to correlation effect in stronger regime; however, with growth in r_c the difference between X-only and correlated energies tends to assume greater significance. In Fig. 2, absolute correlation energy with respect to r_c are plotted for some selected states. Panels (a), (b) correspond to Wigner and LYP. In both cases, it is noticed that, the nature of correlation energy with compression, maintains similar qualitative pattern for all states, for a given functional. In (a), this contribution is found to amplify steadily with confinement strength from free atom, becoming more prominent in lower r_c . Again, crossing between different states takes place quite frequently at several r_c 's. The qualitative nature of curves is comparable to the recently published results of [74]. For LYP, however, the plot in (b) considerably alters from (a); as r_c reduces from free limit, $E_{\text{corr}}^{\text{LYP}}$ lowers sharply until reaching a minimum,

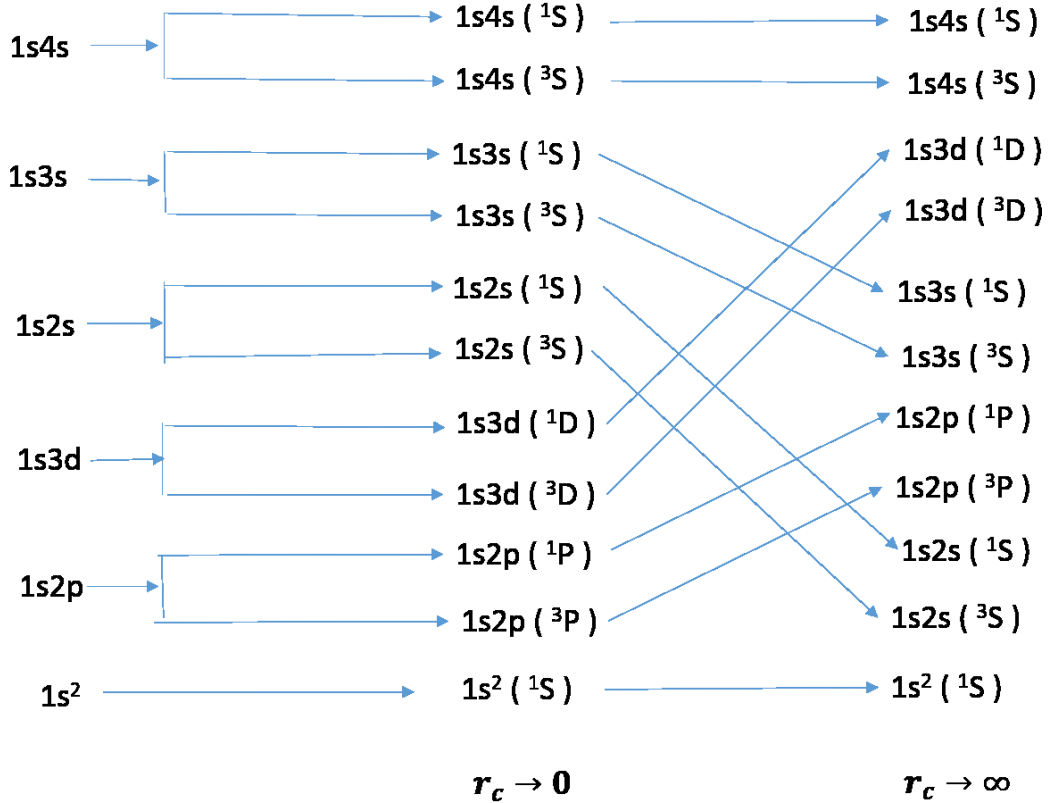


FIG. 3: Correlation diagram for a He atom in an impenetrable spherical cavity of radius r_c .

and then it goes up quite dramatically at certain r_c . Here also few crossovers found, which, again however, alone can not adequately explain the observed crossing pattern in energies.

The interplay between ordering and crossing of states as functions of r_c , may be analyzed by constructing a traditional correlation diagram, widely used in quantum chemistry [30]. Besides the states of previous tables, here we also include 1s3s and 1s4s $^3,^1S$. These are ordered according to their energies in the limit $r_c \rightarrow 0$ and $r_c \rightarrow \infty$ in middle and right segments. This diagram in Fig. 3 consists of three columns, left most of which represents two independent particles inside a small sphere. Considering this model to be a starting point, energy ordering for states of confined He within a small cavity ($r_c \rightarrow 0$) and free atom ($r_c \rightarrow \infty$) can be represented as in second and third columns. In the former case, main contribution to energy is provided by kinetic energy, while Coulombic repulsion makes a contribution that is large in absolute value, but small in comparison to kinetic energy. The energies and wave functions for a particle in a rigid sphere are available in standard text book [75]. For a system of two independent particles, energy of a state having configuration $nl, n'l'$, is given by a sum of orbital energies. This simplistic energy-level structure is,

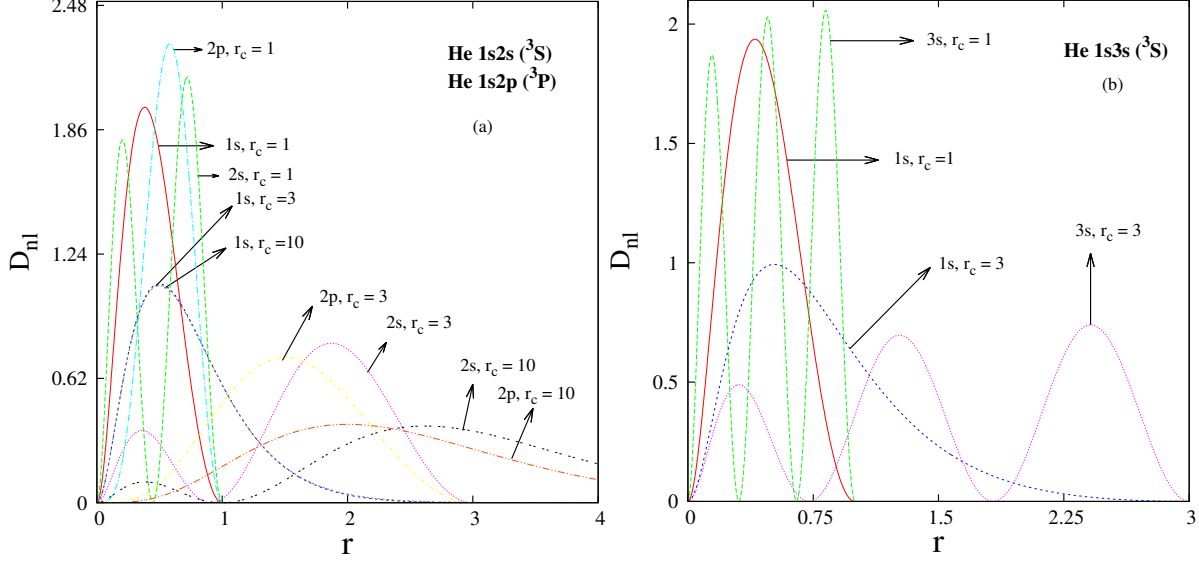


FIG. 4: Radial density of orbitals of confined He, at few r_c 's in various states: (a) $1s2s\ ^3S$ and $1s2p\ ^3P$ (b) $1s3s\ ^3S$. See text for details.

however, complicated in presence of an external potential due to a positive nucleus of charge Z at the center of cavity. In contrast to the one-electron states of particle inside a sphere, for the atomic case, ordering of states does not necessarily remains same at all r_c values. Due to this term in the Hamiltonian, triplet and singlet energies separate out, which is shown in mid-section ($r_c \rightarrow 0$). For the limiting case $r_c \rightarrow \infty$, the energy levels are clearly reordered from its confined counterpart. In this scenario, our ordering matches nicely with that observed in experiment [76]. The transition from confinement to free case leads to interesting degeneracy points in correlation diagram as an outcome of rearrangement of states. The confinement radius for intersection point cannot be defined from the correlation diagram directly. For all states under consideration, the diagram bears qualitative resemblance to that reported in [30] utilizing a highly accurate, correlated wave function.

In order to get an estimate of the above crossings among states with changes in r_c , in Table IV, as an illustration, we present total X-only energy differences, ΔE , between ($1s2p\ ^3P$, $1s2s\ ^3S$) and ($1s3d\ ^3D$, $1s2s\ ^3S$) pair of states along with various contributions, *viz.*, kinetic (ΔT), electron-nucleus (ΔV_{en}) and electron-electron (ΔV_{ee}) at few selected r_c . Proceeding from left to right, one approaches stronger confinement to free atom. A change of sign occurs in energy difference for (3P , 3S) and (3D , 3S) in the ranges of $r_c = 4.5$ – 4.4 and $r_c = 1.1$ – 1.0 , respectively, indicating a crossover between respective multiplet pairs. For a given state, as r_c diminishes, so do both average electron-nucleus and electron-electron

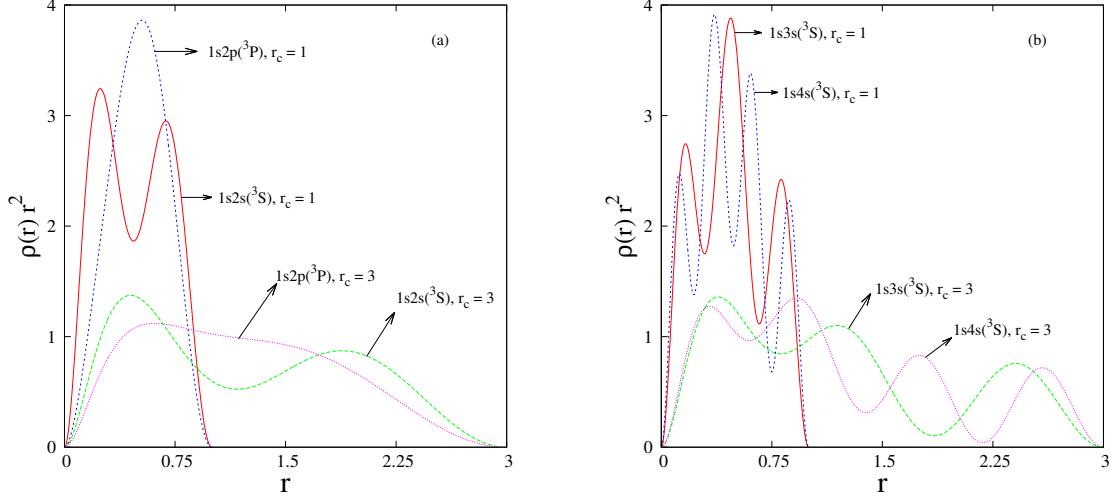


FIG. 5: Radial density of (a) $1s2s\ ^3S$ and $1s2p\ ^3P$ (b) $1s3s\ ^3S$ and $1s4s\ ^3S$ states of confined He at $r_c = 1$ and 3 respectively. Consult text for more details.

distances. This results in a lowering of V_{en} , and increase in magnitude of V_{ee} . Also, as a consequence of uncertainty principle, as the atom is enclosed in progressively smaller box, T tends to accumulate. The relative contribution of each of these terms depends on r_c and the particular state under consideration. The competing effects of these quantities lead to the desired crossing between various multiplets of Fig. 3; major contribution comes from one-electron energies T and V_{en} . An analysis of these components helps us conclude that for free atom as well as for some sufficiently high r_c , ΔV_{en} is responsible for lower energy of 3S than 3P and 3D . For first pair, it is seen that, at $r_c = 20$ or so, higher T of 3S ($\Delta T < 0$) gets compensated by comparable values of V_{en} and V_{ee} of 3P . In the second pair, for certain r_c , V_{en} also compensates the high V_{ee} ; thus at $r_c = 30$, though T and V_{ee} both are higher for 3S than 3D , V_{en} is responsible for (+)ve value of ΔE . As we approach stronger confinement, one notices, for these pairs, ΔV_{ee} hardly contributes to ΔE relative to ΔT and ΔV_{en} . A competition between ΔT and ΔV_{en} determines the ordering between terms; V_{en} is higher for 3S than both 3P , 3D , but a rapid increase of T for 3S compared to other states, leads to the crossing of levels. Another point to be noted is that the data presented in this table is consistent with the correlation diagram of Fig. 3; in free limit, ΔE between $1s2p\ ^3P$, $1s2s\ ^3S$ is lower than the same between $1s3d\ ^3D$, $1s2s\ ^3S$, but due to crossover this pattern changes, and in the opposite limit (e.g., $r_c = 0.1$), ΔE of former pair exceeds that of latter.

Next, in Fig. 4, we plot the radial probability distribution $D_{nl} = r^2 R_{nl}^2(r)$, for $1s$, $2s$, $2p$ orbitals associated with $1s2s\ ^3S$ and $1s2p\ ^3P$ states in panel (a), at r_c 1, 3, 10. Similarly

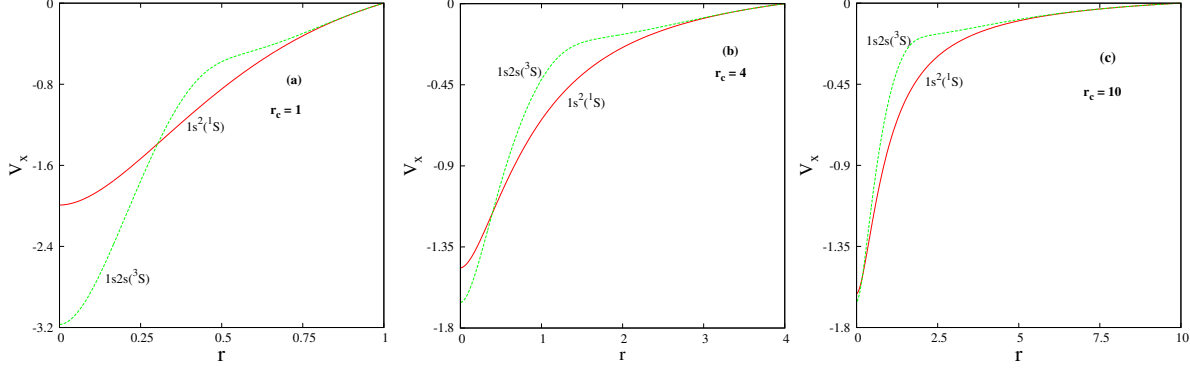


FIG. 6: Exchange potential in first singlet and triplet states of confined He at $r_c = 1, 4, 10$. in panels (a), (b), (c) respectively. See text for details.

(b) gives for 1s, 3s orbitals related to $1s3s\ ^3S$, at r_c 1 and 3. As expected, confinement effects are rather pronounced for outermost orbitals in comparison to other orbitals. Thus one notices that 2s, 2p, 3s densities modify significantly as the atom is squeezed at high pressure. At high r_c (10), area under the first peak of 2s is negligible, resulting in radial density of 2s, 2p orbitals being quite similar. As confinement strengthens, latter two orbitals begin to differ from each other. Now the area of 2s orbital assumes significance relative to its free limit, while the maximum of $D_{2p}(r)$ lies in between two maxima of 2s density. For 1s orbital, at $r_c = 3$ and 10, two curves almost overlap, and as we proceed to smaller r_c (1), the positions of maxima remain almost unaltered while height of the peaks extend. The difference between confined and unconfined charge distributions for 2s, 2p orbitals shows distinct changes. The position of nodes and local maxima are shifted to lower r 's and magnitudes become considerably larger. This phenomenon is more prominent for orbitals in (b) having larger number of nodes than 2s. Thus, in passing from $r_c = 3$ (weak) to 1 (strong), 1s orbital records a change in peak height, without much shift in its position, while for 3s, in going from $r_c = 3$ to 1, significant variations take place in nodal positions, as well as magnitude of local maxima. Hence, it is reasonable to assume that, the crossing of energy levels as discussed earlier, may be attributed mainly to adjustment of outermost orbitals, since inner orbitals change rather slowly, as pressure goes up.

The effect of pressure on radial densities is nicely depicted in Fig. 5: panel (a) shows this for $1s2p\ ^3P$ and $1s2s\ ^3S$, while (b) for $1s3s\ ^3S$ and $1s4s\ ^3S$, respectively, at two representative r_c , namely, 1 and 3. One notices 4, 3, 2 and 1 maxima in $1s4s$, $1s3s$, $1s2s$ and $1s2p$ states. For a given state, with increasing pressure, the positions of these maxima get shifted to

TABLE V: Density moments (X-only) of $1s^2$ (1S), $1s2s$ (3S) states of confined He at various r_c 's. Numbers in the parentheses denote literature results. See text for details.

r_c	$1s^2$ 1S						$1s2s$ 3S					
	$\langle \frac{1}{r^2} \rangle$	$\langle \frac{1}{r} \rangle$	$\langle r \rangle$	$\langle r^2 \rangle$	$\langle r^3 \rangle$	$\langle r^4 \rangle$	$\langle \frac{1}{r^2} \rangle$	$\langle \frac{1}{r} \rangle$	$\langle r \rangle$	$\langle r^2 \rangle$	$\langle r^3 \rangle$	$\langle r^4 \rangle$
0.1	1866.493	49.550	0.099	0.005	0.0003	0.00002	2865.944	56.171	0.099	0.005	0.0004	0.00003
0.3	228.700	17.099	0.290	0.048	0.008	0.001	342.610	19.183	0.295	0.053	0.010	0.002
0.5	91.406	10.653	0.473	0.128	0.038	0.012	133.083	11.807	0.486	0.145	0.0184	0.017
0.8	42.305	7.088	0.727	0.308	0.145	0.073	58.561	7.685	0.765	0.362	0.192	0.109
1.0	30.532	5.934	0.883	0.459	0.266	0.167	40.703	6.326	0.945	0.556	0.368	0.260
			(0.883 ^{a,b})	(0.460 ^a , 0.459 ^b)	(0.267 ^a , 0.267 ^b)	(0.168 ^a , 0.167 ^b)						
4.0	12.081	3.393	1.829	2.271	3.523	6.484	9.510	2.645	3.024	6.494	16.232	43.767
			(1.831 ^{a,b})	(2.272 ^{a,b})	(3.525 ^a , 3.524 ^b)	(6.458 ^a , 6.456 ^b)						
5.0	12.025	3.380	1.848	2.346	3.785	7.393	8.913	2.501	3.498	9.069	27.639	91.174
			(1.850 ^{a,b})	(2.349 ^{a,b})	(3.790 ^a , 3.789 ^b)	(7.371 ^a , 7.366 ^b)						
8.0	12.019	3.378	1.852	2.363	3.858	7.717	8.442	2.353	4.472	16.324	71.987	349.170
			(1.855 ^{a,b})	(2.370 ^a , 2.369 ^b)	(3.880 ^a , 3.878 ^b)	(7.765 ^a , 7.756 ^b)						
∞	12.0	3.37 ^c	1.851 ^c	2.362 ^c	3.85	7.70	8.365	2.318	4.994	21.914	122.04	786.72
			(1.855 ^{a,b})	(2.373 ^a , 2.372 ^b)	(3.891 ^a , 3.886 ^b)	(7.803 ^a , 7.777 ^b)						

^aHF result [50].

^bZMP result [50].

^cThe corresponding HF result [77], with density normalized to unity, for $\langle \frac{1}{r} \rangle$, $\langle r \rangle$ and $\langle r^2 \rangle$ are 1.1544, 2.5599 and 11.5612. Present estimates are: 1.1578, 2.5030, 11.0112.

lower r , peaks become narrower and enhance in magnitude.

To pursue further, it is worthwhile to study the performance of present exchange potential. It has been compared with other accurate potentials in literature, which reproduce HF electron density. Some such examples are BJ model potential, ZMP, B88 and $SC\alpha$ -LDA method. As such, $v_x(r)$ is calculated at each point within the work-function approximation, by solving the KS equation self-consistently for a given r_c . In Fig. 6, it is displayed at three r_c values (1, 4, ∞), for ground and $1s2s$ (3S) states of He. Its behavior in confined environment is visibly different from that in the free limit; with lowering of r_c it becomes steeper. For 3S state there is a distinct hump in the curve, which gets flatter with a reduction in confinement strength. An analysis of [50] reveals that, BJ and ZMP potentials perform quite well in reproducing the exact exchange for a two-electron confined system in ground

TABLE VI: Ground-states energies of Li^+ and Be^{2+} in spherical cavity of various r_c 's.

r_c	Li^+				Be^{2+}			
	X-only	XC-Wigner	XC-LYP	Literature	X-only	XC-Wigner	XC-LYP	Literature
0.5	11.8249 11.82550 ^a	11.7234	11.9715	11.7790 ^b , 11.7768 ^c , 11.76771 ^d	0.1525 0.15261 ^a	0.0492	0.2767	0.1078 ^b , 0.1056 ^c , 0.10801980 ^d
0.6	3.9733 3.97368 ^a	3.8798	4.0774	3.9284 ^b , 3.9262 ^c , 3.9934290 ^d	-6.1964 -6.19641 ^a	-6.2923	-6.1153	-6.2402 ^b , -6.2423 ^c , -6.288159 ^d , -6.242352 ^e
0.7	-0.3149 -0.31480 ^a	-0.4019	-0.2422	-0.3590 ^b , -0.3611 ^c , -0.361136 ^e	-9.4540 -9.45401 ^a	-9.5441	-9.4046	-9.4970 ^b , -9.4991 ^c , -9.499124 ^e
0.8	-2.8178	-2.8996	-2.7692	-2.8612 ^b , -2.8632 ^c , -2.893898 ^d , -2.863228 ^e	-11.2234	-11.3091	-11.1979	-11.2658 ^b , -11.2679 ^c , -11.26839 ^d , -11.267912 ^e
0.9	-4.3490 -4.34907 ^a	-4.4265	-4.3192	-4.3918 ^b , -4.3937 ^c , -4.393732 ^e	-12.2204 -12.22028 ^a	-12.3027	-12.2131	-12.2624 ^b , -11.2645 ^c
1.0	-5.3183 -5.31832 ^a -5.318324 ^f	-5.3922	-5.3033	-5.3605 ^b , -5.3635 ^g , -5.3624 ^c , -5.362399 ^{e,f}	-12.7954 -12.79481 ^a	-12.8750	-12.8021	-12.8369 ^b , -12.8393 ^c , -12.839307 ^e
1.2	-6.3632 -6.36317 ^a	-6.4318	-6.3698	-6.4047 ^b , -6.4065 ^c , -6.407358 ^d	-13.3295 -13.32825 ^a	-13.4057	-13.3550	-13.3701 ^b , -13.3733 ^c , -13.36396 ^d
1.4	-6.8302 -6.82981 ^a	-6.8953	-6.8509	-6.8713 ^b , -6.8732 ^c , -6.855290 ^d	-13.5151 -13.51486 ^a	-13.5894	-13.5515	-13.5552 ^b , -13.5590 ^c , -13.556580 ^d
1.6	-7.0462 -7.04585 ^a	-7.1090	-7.0761	-7.0869 ^b , -7.0892 ^c	-13.5791 -13.57911 ^a	-13.6526	-13.6215	-13.6193 ^b , -13.6232 ^c
1.8	-7.1475 -7.14643 ^a	-7.2089	-7.1834	-7.1880 ^b , -7.1906 ^c , -7.192726 ^d	-13.6007 -13.60028 ^a	-13.6738	-13.6465	-13.6415 ^b , -13.6449 ^c , -13.639290 ^d
2.0	-7.1952 -7.19460 ^a	-7.2556	-7.2348	-7.2356 ^{b,g} , -7.2383 ^c , -7.238402 ^e	-13.6079 -13.61002 ^a	-13.6808	-13.6555	-13.6493 ^b , -13.6521 ^c
2.5	-7.2306	-7.2901	-7.2750	-7.2740 ^c , -7.258839 ^d	-13.6110	-13.6838	-13.6611	-13.6553 ^c , -13.654130 ^d
3.5	-7.2362	-7.2955	-7.2836	-7.2791 ^c , -7.279050 ^d	-13.6112	-13.6840	-13.6633	-13.6555 ^c , -13.655678 ^d
5.0	-7.2363 -7.236415 ^f	-7.2956	-7.2852	-7.2784 ^b , -7.2783 ^g , -7.2798 ^c , -7.279254 ^d , -7.279913 ^{e,f}	-13.6112	-13.6840	-13.6644	-13.6539 ^b , -13.6555 ^c , -13.657630 ^d , -13.655566 ^e
7.0	-7.2363	-7.2956	-7.2860	-7.2784 ^b , -7.279913 ^e	-13.6112	-13.6840	-13.6651	-13.6539 ^b , -13.655566 ^e
∞	-7.2363 -7.236415 ^f	-7.2956	-7.2876	-7.2799 ^{g,c} , -7.279913 ^{e,f}	-13.6112	-13.6840	-13.6665	-13.6555 ^c , -13.655566 ^e

^aRef. [26].

^bRef. [9].

^cRef. [19].

^dRef. [27]

^eRef. [23].

^fRef. [21].

^gRef. [11].

state. A comparison of our figure confirms that $v_x(r)$ at $r_c = 4$ qualitatively reproduces the characteristic features found in the literature [50].

Simply looking at $\rho(r)$ plots does not provide a complete picture, as possible deviation between different densities can be sometimes very small compared with modulations in a given density at various r . For this, one resorts to some of the indicators (in the form of

density moments) which quantitatively characterize the density distribution in a compact manner, and offer valuable insights. To this end, six expectation values, $\langle \frac{1}{r^2} \rangle$, $\langle \frac{1}{r} \rangle$, $\langle r \rangle$, $\langle r^2 \rangle$, $\langle r^3 \rangle$, $\langle r^4 \rangle$ are offered for ground (left) and $1s2s\ ^3S$ (right) states of boxed-in He, at nine selected r_c 's within the X-only framework. Only some scattered results are available for $\langle r \rangle$, $\langle r^2 \rangle$, $\langle r^3 \rangle$, $\langle r^4 \rangle$ in ground state, where the obtained moments match excellently with those of ZMP and HF values [50]; in some occasions, they are completely identical. In free atom ground state, numerical HF results [77] for $\langle \frac{1}{r} \rangle$, $\langle r \rangle$, $\langle r^2 \rangle$ compare very nicely with current work. For excited state, no published results could be found, to the best of our knowledge. Hence, the proposed approach offers accurate moments in both confined and free atom.

B. Confined He-isoelectronic series

Now, we aim to analyze the role played by nuclear charge, Z on the properties of atom under varying confinement strengths. In this regard, in Table VI, ground-state energies, without and with effects of correlation, are recorded for two members of He iso-electronic series (Li^+ , Be^{2+}) at representative r_c , along with reference theoretical results, wherever feasible. As expected, for all systems, stronger confinement leads to enhanced total energies. The X-only results of columns 2 and 6 are compared with HF calculation [26] throughout the entire r_c ; also for $Z = 3$, at $r_c = 1, 5$ as well as the free atom, with that of [21]. The agreement with both these references is extremely good. The correlated values of two ionic species, on the other hand, can be compared with CI [9] and various Monte-Carlo [11, 27] methods, in addition to Hylleraas-type [19, 21, 23] results. The general trend is similar to that found for He. At larger r_c , difference between Wigner and LYP remains rather quite small, where both slightly underestimate literature energies. In stronger confinement region, Wigner energies appears to have a marginal edge over LYP. Taking the variational Monte-Carlo [27] as reference, discrepancies appear to be slightly higher in larger r_c . As Z goes up, electron density becomes more contracted; this can be looked as a shrinkage of atomic dimensions due to presence of a (+)ve charge at nucleus, which is akin to the compression of atom. However, the difference between this process and the one created by putting it inside an impenetrable cavity of varying radius is that, by enhancing Z , the pressure is induced centrally, whereas in latter case it is exerted peripherally. This difference is observed in energy pattern as well; the induced pressure due to growing Z eventually lowers the total

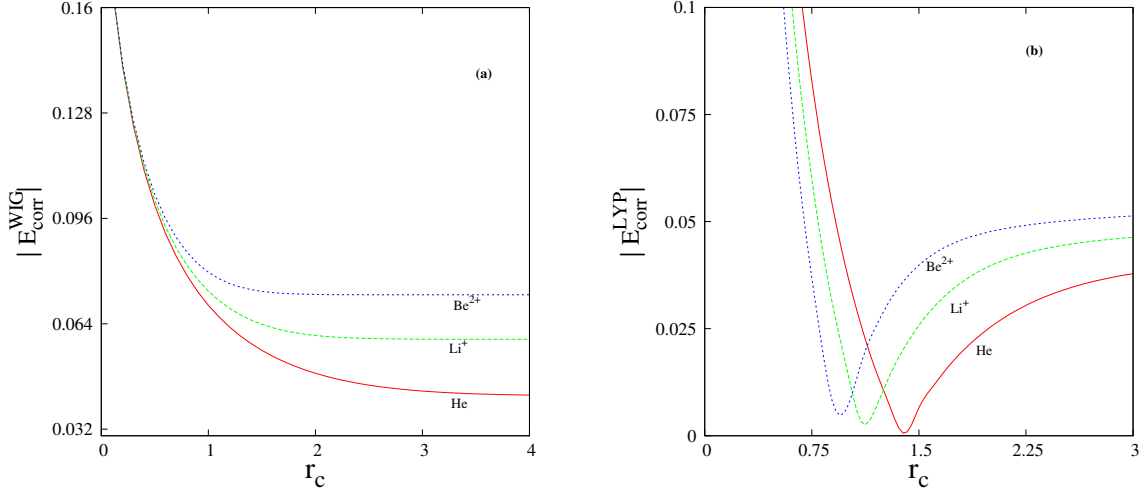


FIG. 7: Absolute correlation energy, with Wigner (a) and LYP (b) functionals, in the lowest states of He, Li^+ and Be^{2+} . See text for details.

energy at a fixed confinement strength.

A few words may now be devoted to the influence of Z on correlation energy as confinement takes place. Thus Fig. 7 depicts how $|E_{\text{corr}}|$, approximated by Wigner and LYP functional, behaves with variation of r_c , in case of ground states of He, Li^+ and Be^{2+} , in panels (a) and (b). Starting from the limiting case of free ion, $E_{\text{corr}}^{\text{WIG}}$, for a given member of iso-electronic series, remains practically unaffected until about $r_c \approx 2$ a.u.; any further compression is accompanied by a sharp increase. As Z passes from 2 to 4, with lowering in r_c , the differences in $E_{\text{corr}}^{\text{WIG}}$ between two successive members reduce. As in stronger confinement regime, both nucleus-electron and electron-electron distances fall down; hence the effect of Z gets dominated by the confining potential. This results in the fact that as r_c declines, the plots very nearly overlap with each other. These observations reinforce the inferences drawn in our recent report [65]. In contrast, however, panel (b) shows a distinct minimum in $E_{\text{corr}}^{\text{LYP}}$ vs r_c graph for all the species. As the cavity gets smaller, its magnitude at first diminishes steadily, then passes through a minimum and ultimately rises abruptly. This minimum is deeper and wider for He than Li^+ , which in turn, has greater measure than Be^{2+} . The position of this minimum moves to lower r_c , as Z advances.

TABLE VII: Ground-state energies of Li and Be, confined at the center of an impenetrable spherical cavity of radius r_c . See text for details.

r_c	Li					Be			
	X-only	Literature	XC-Wigner	XC-LYP	Literature	X-only	Literature	XC-Wigner	XC-LYP
0.5	78.4392		78.2803	78.7693		124.2082		123.9863	124.6458
0.6	48.4997		48.3534	48.7539		75.1709		74.9657	75.5088
0.7	31.1262		30.9903	31.3236		46.8218		46.6305	47.0847
0.8	20.2839		20.1567	20.4372		29.1990		29.0193	29.4035
1.0	8.2385	-8.5139 ^a	8.1249	8.3285		9.7334	9.7327 ^b , 9.8351 ^c	9.5720	9.8537
1.2	2.2191	2.2191 ^d	2.1155	2.2663		0.0917	0.1368 ^e	-0.0560	0.1550
1.5	-2.2278	-2.2281 ^b ,	-2.3208	-2.2221	-1.9085 ^c ,	-6.9464	-6.9477 ^b ,	-7.0796	-6.9391
					-1.9870 ^g		-6.92237 ^e		
2.0	-5.1780	-5.1782 ^b ,	-5.2606	-5.2099	-5.1305 ^c ,	-11.5064	-11.5079 ^b ,	-11.6244	-11.5503
		-5.1780 ^d ,			-5.1251 ^g		-11.4895 ^e		
		-5.0841 ^a					-11.5078 ^f		
2.5	-6.2951	-6.2955 ^d	-6.3721	-6.3451		-13.1567	-13.1583 ^b ,	-13.2660	-13.2261
							-13.1583 ^f ,		
							-13.1413 ^e		
3.0	-6.8018	-6.8027 ^b	-6.8753	-6.8609	-6.8304 ^c ,	-13.8614	-13.8613 ^b ,	-13.9651	-13.9441
		-6.7463 ^a ,			-6.8297 ^g		-13.8631 ^f ,		
		-6.8026 ^d					-13.8468 ^e		
4.0	-7.2035	-7.2046 ^b ,	-7.2731	-7.2694	-7.2448 ^c ,	-14.3670	-14.3685 ^b ,	-14.4645	-14.4606
		-7.1859 ^a ,			-7.2442 ^g		-14.3678 ^f ,		
							-14.3521 ^e		
5.0	-7.3383	-7.3395 ^b ,	-7.4060	-7.4058	-7.3815 ^c ,	-14.5080	-14.5091 ^b ,	-14.6024	-14.6046
		-7.3230 ^a ,			-7.3815 ^g		-14.4918 ^e		
		-7.2045 ^d							
6.0	-7.3913	-7.3925 ^b	-7.4577	-7.4588	-7.4342 ^c ,	-14.5515	-14.5522 ^b ,	-14.6443	-14.6488
		-7.3769 ^a			-7.4343 ^g		-14.5345 ^e		
8.0	-7.4238	-7.4249 ^b ,	-7.4890	-7.4903	-7.4658 ^c ,	-14.5695	-14.5535 ^e ,	-14.6612	-14.6672
		-7.4098 ^a ,			-7.4657 ^g		-14.5704 ^b		
		-7.4246 ^d							
10.0	-7.4301	-7.4717 ^b ,	-7.4948	-7.4962		-14.5711	-14.5729 ^f ,	-14.6626	-14.6692
		-7.4165 ^a					-14.5567 ^e		

^aRef. [78]

^bRef. [8]

^cRef. [28]

^dRef. [34]

^eRef. [79]

^fRef. [80]

^gRef. [15]

C. Confined Li and Be atoms

Finally, we use our method to study more than two-electron systems; as sample cases we present the results for Li and Be atoms confined in an impenetrable sphere. The results for this confined three- and four-electron systems respectively, are reported for both X-only

and correlated cases separately in Table VII for ground state. For sake of comparison, along with our X-only results of Li in column 2, we provide the results from HF [8], direct variational [78] and POEP methods [34] in column 3. As it is visible from the table, reference results are more prevalent in the region $r_c \geq 1$ than $r_c \leq 1$. The presented data for our X-only calculation are in excellent agreement with those of [8]. Comparison with [78] and [34] also show good matching. The correlated energies can be compared with variational Monte Carlo method [28] and Rayleigh-Ritz variational approach [15]. For both functionals, with decreasing value of r_c the difference between present and reference energy tends to accumulate. Furthermore, at smaller r_c region, Wigner and LYP differ from each other significantly. Results reported for X-only energy values for Be atom are also in very good harmony with HF results of [8, 80]. No correlated results could be found in literature for confined Be. Also all the mentioned references are of wave function based method; no DFT calculation of these systems are found.

IV. CONCLUDING REMARKS

A simple general and accurate KS DFT method has been proposed for calculation of an atom enclosed inside a rigid spherical cavity of varying radius. The prescription is computationally feasible and can be easily extended to other atoms/states. Properties such as energy, radial density, expectation values are reported for ground and singly excited states ($1s2s\ ^3S$, $1s2p\ ^3P$, $1s3d\ ^3D$) of He, as well as ground states of Li^+ , Be^{2+} , in weak, intermediate, strong confinement strengths. Moreover, ground state results are also reported for Li and Be atoms. The overall agreement with existing literature data is excellent for the entire region, with X-only results being very close to HF. An analysis of energy ordering is offered in terms of traditional correlation diagram, and individual energy components.

To the best of our knowledge, this is the first reporting of excited state of confined atoms in very strong confinement ($r_c \leq 0.5$) region, excepting the work of [45], which published results for ground and singly excited ($1s2s\ ^3S$, up to $r_c = 2$) states of He. The correlation contribution to energy in smaller box ($r_c \leq 1$) is rather less dramatic than in a free atom. Thus, it is possible to obtain quite accurate results for a given state, provided the exchange contribution is properly accounted for, which, of course, lies behind the general success of this approach. The two correlation functionals (Wigner and LYP) behave quite differently

as box size is changed. In the former, its magnitude gradually increases with confinement strength, whereas LYP shows a reduction until the appearance of a minimum at a certain r_c , followed by a steep rise. In free limit, LYP appears to perform better than Wigner. In the opposite limit, however, Wigner seems to have an edge over LYP, reflecting a trend which is qualitatively similar to that observed in literature. Confinement induces interesting energy level crossings, in conformity with Hund's rule. When pressure enhances, the asymptotic behavior of states are greatly affected; energy level goes from an atomic mean field theory ($r_c \rightarrow \infty$) to particle in a hard-sphere model ($r_c \rightarrow 0$). These crossings are mainly attributed to X-only energy. For more accurate results, better correlation energy functionals need to be designed and employed; one such functional reported in [51] is currently being pursued by us. Further application of the method is being made to other atoms as well as more realistic confinement scenario (such as *soft or penetrable* potentials). The results on these works are as encouraging as reported here. However to limit the size of this article, it appears prudent to communicate them separately in future. It would also be worthwhile to further probe the critical radii (r_c where energies become zero), influence of electric and magnetic field through dynamical study, information theoretical analysis, etc.

V. ACKNOWLEDGEMENT

SM is grateful to IISER Kolkata for a Senior Research Fellowship. AKR gratefully acknowledges BRNS, Mumbai, India (sanction order: 58/14/03/2019-BRNS/10255) for financial support. We thank Dr. Neetik Mukherjee for giving a critical reading of the manuscript.

-
- [1] W. Jaskólski, Phys. Rep. **271**, 1 (1996).
 - [2] J. Sabin, E. Brändas, and S. Cruz (Eds.), *Adv. Quant. Chem.*, vol. 57 & 58 (Academic Press, New York, 2009).
 - [3] K. D. Sen (Ed.), *Electronic Structure of Quantum Confined Atoms and Molecules* (Springer International Publishing, Switzerland, 2014).
 - [4] E. Ley-Koo, Revista Mexicana de Física **64**, 326 (2018).
 - [5] A. Michels, J. de Boer, and A. Bijl, Physica **4**, 981 (1937).
 - [6] B. L. Burrows and M. Cohen, Int. J. Quant. Chem. **106**, 478 (2006).

- [7] C. A. Ten Seldam and S. R. De Groot, *Physica* **18**, 891 (1952).
- [8] E. V. Ludeña, *J. Chem. Phys.* **69**, 1770 (1978).
- [9] E. V. Ludeña and M. Gregori, *J. Chem. Phys.* **71**, 2235 (1979).
- [10] R. Rivelino and J. D. M. Vianna, *J. Phys. B* **34**, L645 (2001).
- [11] C. Joslin and S. Goldman, *J. Phys. B* **25**, 1965 (1992).
- [12] J. L. Marín and S. A. Cruz, *J. Phys. B* **24**, 2899 (1991).
- [13] A. Banerjee, C. Kamal, and A. Chowdhury, *Phys. Lett. A* **350**, 121 (2006).
- [14] A. Flores-Riveros, N. Aquino, and H. E. Montgomery Jr., *Phys. Lett. A* **374**, 1246 (2010).
- [15] C. Le Sech and A. Banerjee, *J. Phys. B* **44**, 105003 (2011).
- [16] S. Ting-yun, B. Cheng-Guang, and L. Bai-Wen, *Commun. Theor. Phys.* **35**, 195 (2001).
- [17] H. E. Montgomery Jr., N. Aquino, and A. Flores-Riveros, *Phys. Lett. A* **374**, 2044 (2010).
- [18] N. Aquino, A. Flores-Riveros, and J. F. Rivas-Silva, *Phys. Lett. A* **307**, 326 (2003).
- [19] A. Flores-Riveros and A. Rodríguez-Contreras, *Phys. Lett. A* **372**, 6175 (2008).
- [20] C. Laughlin and S. I. Chu, *J. Phys. A* **42**, 265004 (2009).
- [21] C. L. Wilson, H. E. Montgomery Jr., K. D. Sen, and D. C. Thompson, *Phys. Lett. A* **374**, 4415 (2010).
- [22] H. E. Montgomery Jr. and V. I. Pupyshev, *Phys. Lett. A* **377**, 2880 (2013).
- [23] S. Bhattacharyya, J. K. Saha, P. K. Mukherjee, and T. K. Mukherjee, *Phys. Scr.* **87**, 065305 (2013).
- [24] H. E. Montgomery Jr. and V. I. Pupyshev, *Theor. Chem. Acc.* **134**, 1598 (2015).
- [25] J. Saha, S. Bhattacharyya, and T. K. Mukherjee, *Int. J. Quantum Chem.* **116**, 1802 (2016).
- [26] Y. Yakar, B. Çakir, and A. Özmen, *Int. J. Quantum Chem.* **111**, 4139 (2011).
- [27] S. B. Doma and F. N. El-Gammal, *J. Theor. Appl. Phys.* **6**, 28 (2012).
- [28] A. Sarsa and C. Le Sech, *J. Chem. Theory Comput.* **7**, 2786 (2011).
- [29] T. D. Young, R. Vargas, and J. Garza, *Phys. Lett. A* **380**, 712 (2016).
- [30] V. I. Pupyshev and H. E. Montgomery Jr., *Theor. Chem. Acc.* **136**, 138 (2017).
- [31] J. Garza, J. M. Hernández-Pérez, J.-Z. Ramírez, and R. Vargas, *J. Phys. B* **45**, 015002 (2012).
- [32] J. P. Connerade, V. K. Dolmatov, and P. A. Lakshmi, *J. Phys. B* **33**, 251 (2000).
- [33] S. H. Patil, K. D. Sen, and Y. P. Varshni, *Can. J. Phys.* **83**, 919 (2005).
- [34] A. Sarsa, E. Buendía, and F. J. Gálvez, *J. Phys. B* **47**, 185002 (2014).
- [35] J. A. Ludlow and T. G. Lee, *Phys. Rev. A* **91**, 032507 (2015).

- [36] F. J. Gálvez, E. Buendía, and A. Sarsa, *Int. J. Quantum Chem.* **117**, e25421 (2017).
- [37] M.-A. Martínez-Sánchez, M. Rodríguez-Bautista, R. Vargas, and J. Garza, *Theor. Chem. Acc.* **135**, 207 (2016).
- [38] S. F. Vyboishchikov, *J. Comput. Chem.* **37**, 2677 (2016).
- [39] A. L. Buchachenko, *J. Phys. Chem. B* **105**, 5839 (2001).
- [40] V. K. Dolmatov, A. S. Baltenkov, J.-P. Connerade, and S. T. Manson, *Radiat. Phys. Chem.* **70**, 417 (2004).
- [41] W. Grochala, R. Hoffmann, J. Feng, and N. Ashcroft, *Angew. Chem. Int. Ed.* **36**, 3620 (2007).
- [42] R. G. Parr and W. Yang, *Density Functional Theory of Atoms and Molecules* (Oxford University Press, New York, 1989).
- [43] A. D. Becke, *Phys. Rev. A* **38**, 3098 (1988).
- [44] J. Garza, R. Vargas, and A. Vela, *Phys. Rev. E* **58**, 3949 (1998).
- [45] N. Aquino, A. Flores-Riveros, J. F. Rivas-Silva, and K. D. Sen, *J. Chem. Phys.* **124**, 054311 (2006).
- [46] J. P. Perdew and Y. Wang, *Phys. Rev. B* **45**, 13244 (1992).
- [47] J. Garza, R. Vargas, N. Aquino, and K. D. Sen, *J. Chem. Sci.* **117**, 379 (2005).
- [48] A. Borgoo, D. J. Tozer, P. Geerlings, and F. D. Proft, *Phys. Chem. Chem. Phys.* **10**, 1406 (2008).
- [49] S. Waugh, A. Chowdhury, and A. Banerjee, *J. Phys. B* **43**, 225002 (2010).
- [50] S. F. Vyboishchikov, *J. Comput. Chem.* **36**, 2037 (2015).
- [51] S. F. Vyboishchikov, *Chem. Phys. Chem.* **18**, 3478 (2017).
- [52] F.-A. Duarte-Alcaráz, M.-A. Martínez-Sánchez, M. Rivera-Almazo, R. Vargas, R. Rosas-Burgos, and J. Garza, *J. Phys. B* **52**, 135002 (2019).
- [53] M. Lozano-Espinosa, J. Garza, and M. Galván, *Phil. Mag.* **97**, 284 (2017).
- [54] D. Chakraborty and P. K. Chattaraj, *J. Phys. Chem. A* **123**, 4513 (2019).
- [55] V. Sahni and M. Harbola, *Int. J. Quant. Chem. Symp.* **24**, 569 (1990).
- [56] V. Sahni, Y. Li, and M. Harbola, *Phys. Rev. A* **45**, 1434 (1992).
- [57] G. Bruhal and S. M. Rothstein, *J. Chem. Phys.* **69**, 1177 (1978).
- [58] C. Lee, Y. Wang, and R. G. Parr, *Phys. Rev. B* **37**, 785 (1988).
- [59] R. Singh and B. M. Deb, *J. Chem. Phys.* **104**, 5892 (1996).
- [60] A. K. Roy, R. Singh, and B. M. Deb, *J. Phys. B* **30**, 4763 (1997).

- [61] A. K. Roy, R. Singh, and B. M. Deb, *Int. J. Quant. Chem.* **65**, 317 (1997).
- [62] A. K. Roy and S. I. Chu, *Phys. Rev. A* **65**, 052508 (2002).
- [63] A. K. Roy, *J. Phys. B* **37**, 4369 (2004).
- [64] A. K. Roy, *J. Phys. B.* **38**, 1591 (2005).
- [65] S. Majumdar and A. K. Roy, *Quant. Rep.* **2**, 189 (2020).
- [66] A. K. Roy, *Phys. Lett. A* **321**, 231 (2004).
- [67] A. K. Roy, *J. Phys. G* **30**, 269 (2004).
- [68] T. Ziegler, A. Rauk, and E. J. Baerends, *Thero. Chim. Acta* **43**, 261 (1977).
- [69] B. M. Gimarc, *J. Chem. Phys.* **47**, 5110 (1967).
- [70] P. A. M. Dirac, *Proc. Camb. Phil. Soc.* **26**, 376 (1930).
- [71] A. Luzón, E. Buendía, and F. J. Gálvez, *Int. J. Quantum Chem.* **120**, e26048 (2020).
- [72] A. Sarsa, E. Buendía, F. J. Gálvez, and J. Katriel, *Chem. Phys. Lett.* **702**, 106 (2018).
- [73] S. H. Patil and Y. P. Varshni, *Can. J. Phys* **82**, 647 (2004).
- [74] A. Sarsa, E. Buendía, and F. J. Gálvez, *J. Phys. B.* **49**, 145003 (2016).
- [75] S. Flügge, *Practical quantum mechanics I* (Springer, Berlin, 1971).
- [76] J. E. Sansonetti and W. C. Martin, *J. Phys. Chem. Ref. Data* **34**, 1559 (2005).
- [77] C. F. Fischer, *The Hartree-Fock Method For Atoms* (Wiley, New York, 1977).
- [78] A. D. Sañu-Ginartea, E. M. Guillén-Romeroa, L. Ferrer-Galindob, L. A. Ferrer-Moreno, R. Betancourt-Riera, and R. Riera, *Results in Phys.* **13**, 102261 (2019).
- [79] A. D. Sañu-Ginartea, L. Ferrer-Galindob, R. A. Rossa, A. Corella-Madueño, R. Betancourt-Riera, L. A. Ferrer-Moreno, and R. Riera, *J. Phys. Commun.* **2**, 015001 (2018).
- [80] M. Rodríguez-Bautista, C. Díaz-García, A. M. Navarrete-López, R. Vargas, and J. Garza, *J. Chem. Phys.* **143**, 034103 (2015).

